Giant, 28, 2026, 100391

Full-length article

Comparative study investigating bio-based reactive diluents for photo-curing applications

Vojtěch Jašek[a,*], Otakar Bartoš[b], Jan Prokeš[b], Silvestr Figalla[a], Radek Přikryl[a]

[a] Institute of Materials Chemistry, Faculty of Chemistry, Brno University of Technology, Brno 612 00, Czech Republic
[b] Materials Research Centre, Faculty of Chemistry, Brno University of Technology, Brno 612 00, Czech Republic

Keywords: Reactive diluents, NMR, Viscosity, Reactivity, Flexural tests, Bio-based compounds

This investigation provides a comprehensive comparison of the selected and synthesized bio-based curable compounds used in the photocured methacrylated vegetable oil. The chosen reactive diluents are vanillin methacrylate (VMA), cinnamyl methacrylate (CMA), isosorbide dimethacrylate (IDMA), glycerol methacrylate (GMA), and glycerol trimethacrylate (GTMA). We synthesized all the mentioned compounds with high final yields (>85 %) except for GMA (reached 72 % yield). The structural characterization was provided by ^{1}H NMR and FTIR. In total, four different functional properties were studied: polymerization reactivity, rheological profile, thermal stability, and mechanical characteristics. The most reactive compound, GMA, achieved the polymerization activation energy of 68.2 kJ/mol. The lowest observable viscosity was observed for the curable system containing CMA (25 % in the methacrylated oil), with an apparent viscosity of 405 mPa·s at 25 °C. The most thermally stable system comprised 25 % GTMA in the methacrylated oil, reaching the heat-resistant index of 184 °C. The highest flexural modulus was reached by the GTMA-involving system (596 ± 38 MPa), while the highest flexural strength was reached by the IDMA-involving resin (12.7 ± 0.3 MPa). The best rigid-enhanced system contained 25 % IDMA, while the most tremendous increase in flexibility was observed with resin containing 25 % of VMA.

1 Introduction

The reactive curable systems have been widely used in several chemical industries and material applications, ranging from the small produced objects (dental composites, 3D printed prototypes, and micro components for electronics) [1–3] to the large industrially relevant products (automotive composite parts, reactive adhesives and coatings, and building multi-component materials) [4–6]. Currently, high-performing precursors, mainly derived from fossil-based sources, are used for most applications [7]. Particular polymerizable systems applied in dental composites or 3D printed engineered prototypes are commercially available methacrylates and acrylates, such as ethylene glycol dimethacrylate (EGDMA) [8], ethylene glycol diacrylate (EGDA) [9], 2-hydroxyethyl methacrylate (HEMA) [10], bisphenol A-glycidyl methacrylate (Bis-GMA) [11], or triethylene glycol dimethacrylate (TEGDMA) [12]. The target physical-chemical properties are essential for the required application; therefore, the market offers both rigid/hard thermoset-forming

* Corresponding author.
E-mail address: xcjasekv@vutbr.cz (V. Jašek).
Received 28 December 2025; Received in revised form 13 February 2026; Accepted 2 March 2026

 https://doi.org/10.1016/j.giant.2026.100391

reactive systems (modified bisphenol A and ethylene glycol) and flexible/soft cured resins (modified poly(ethylene glycol) and poly(propylene glycol)) [13,14]. Regarding industrially relevant thermoset precursors, overall costs and the availability of the used compound are the most important factors for producers [15]. Typically, the unsaturated polyester precursors (UPE/UPR) or vinyl ester resins (containing bisphenol A or urethanes) represent the main high-viscosity components [16–18], which are mixed with reactive diluents, such as styrene, methyl methacrylate (MMA), isobornyl acrylate (IBOA), and isobornyl methacrylate (IBOMA), to regulate their eventual characteristics and primarily their rheological properties [19–21]. Most of the mentioned reactive systems perfectly fulfill their purposes effectively in the selected applications, but their chemical production is associated with an unsustainable approach and the use of non-renewable feedstock [22].

Bio-based reactive systems are attracting significant attention as potential renewable substitutes for the precursors currently used in material applications [23]. The production of such materials has rapidly grown over the last 20 years. Regarding the bio-based coating precursors, the forecasted growth reaches 29.4 billion USD by 2032 [24]. The incorporation of renewable carbon into material precursors and systems, the potential reduction of CO_2 emissions, or the limitation of VOCs are the particular motivations for enhancing the sustainable chemical industry [25,26]. Several suggested polymerizable compounds and systems possess high bio-based carbon content in their structures. The specific molecules described in the literature contain substantial bio-based carbon content, which meets the projected sustainability expectations [27–30]. The systems, such as the methacrylated fatty acids (bio-based content: ~63 %) [27], methacrylated eugenol (bio-based content: 71.4 %) [28], or isobornyl methacrylate (bio-based content: 71.4 %) [29] were investigated and described in the literature as the appropriate alternatives to the entirely fossil-based reactive compounds. The regulation of the eventual properties is achievable similarly to the petroleum-derived precursors – flexible systems typically involve fatty acid derivatives with long carbon chains [27,30,31], while the rigid systems are produced from multi-functional short-chain entering molecules (pentaerythritol, sorbitol, bio-based propylene glycol) [30,32–34]. The VOCs generated during material applications, usually from volatile compounds such as styrene or MMA, increase environmental and health hazards during manufacture [35]. Several non-volatile bio-based systems and molecules were proposed and characterized in the literature (modified triacylglycerides, sorbitol polyglycidyl ether, or numerous lignin-based compounds) [35], while some of the commercially available bio-based low-molecular compounds possess similar high volatility as styrene/MMA (isobornyl acrylate of isobornyl methacrylate) [36,37]. Nevertheless, the specific application must select a suitable bio-based alternative based on all key market factors, such as material availability, handling characteristics, and final profitability.

This work presents a comprehensive comparative study involving the synthesis of methacrylated vegetable oil, a bio-based, highly viscous, curable system. Numerous reactive diluents from renewable sources were synthesized and incorporated into the oil-based mixture, including vanillin methacrylate (VMA), cinnamyl methacrylate (CMA), isosorbide dimethacrylate (IDMA), glycerol methacrylate (GMA), and glycerol trimethacrylate (GTMA). We investigated the products' reactivity using Kissinger's theory. Then, we formulated the curable mixtures from modified oil, a particular enhancing compound, and the photoinitiator, and described their flow characteristics to verify the diluting factor. We processed the prepared resins by MSLA 3D printing to obtain solid cured thermosets. Eventually, we studied the thermal stability and mechanical properties of the 3D-printed specimens to characterize the material's performance. The studied properties were evaluated, and the best-performing system, demonstrating significant sustainability, was selected as the optimal bio-based alternative to the currently used compounds in this material field.

2 Experimental section

2.1 Materials

Epoxidized vegetable oil Drapex 39 (epoxidized vegetable oil, OOC: ~6.5 %) was purchased from Ataman Chemicals (Turkey). All other used reactants and substances, methacrylic acid (MA, 99 % stab. 250 ppm MEHQ), methacrylic anhydride (MAAH, 98 % stab. 2000 ppm topanol A), vanillin (97 %), cinnamyl alcohol (98 %), isosorbide (98 %), glycerol (99 %), sodium hydroxide (98 %), ethyl acetate (99 %), potassium acetate (99 %), triethylamine (99 %), anhydrous sodium sulfate (99 %), *tert*–butyl Peroxide (Luperox DI, 98 %), photoinitiator phenylbis(2,4,6-trimethylbenzoyl)phosphine oxide (BAPO, 98 %), and the solvent for NMR analyses d-chloroform ($CDCl_3$, 99.8 atom % D, 0.03 % (v/v) TMS) were obtained from Merck Ltd. (Czech Republic).

2.2 Structural analyses

Nuclear magnetic resonance (NMR) analysis was performed with Bruker Avance III 500 MHz (Bruker, Billerica, MA, USA). The measuring frequency was 500 MHz for ^{1}H NMR. The measurements were performed at 30 °C using D-chloroform ($CDCl_3$) as the solvent with tetramethylsilane (TMS) as the internal standard. The chemical shifts (δ) are expressed in parts per million (ppm) units, referenced by a solvent. Coupling constant (J) is expressed with frequency unit (Hz), with coupling expressed as s-singlet, d-doublet, t-triplet, q-quartet, p-quintet, m-multiplet.

Fourier-transform infrared spectroscopy (FT-IR) was used to determine the functional groups. Analyses were conducted by Bruker Tensor 27 (Billerica, MA, USA) and the attenuated total reflectance (ATR) method. Diamond served as a dispersion component. A diode laser was the irradiation source in this spectroscope. The Michelson interferometer was used to quantify the signal. Spectra comprised 32 scans, with a resolution of 2 cm^{-1}.

Acid number (A.N.) was used to determine the purity of the synthesized compounds. The analysis was performed according to the norm ASTM D974.

2.3 Synthesis of methacrylated oil

Epoxidized vegetable oil (1000 g, OOC 6.5 %, 4 molar equiv. of the reactive epoxide) was poured into a 2000 mL round-bottom flask and mixed with methacrylic acid (387 g, 4.5 mol). The solution was heated to the reaction temperature (120 °C). Then, the catalyst (triethylamine, 15 g, 0.15 mol) was added. The nucleophilic substitution reaction (see Fig. 1) lasted 10 h.

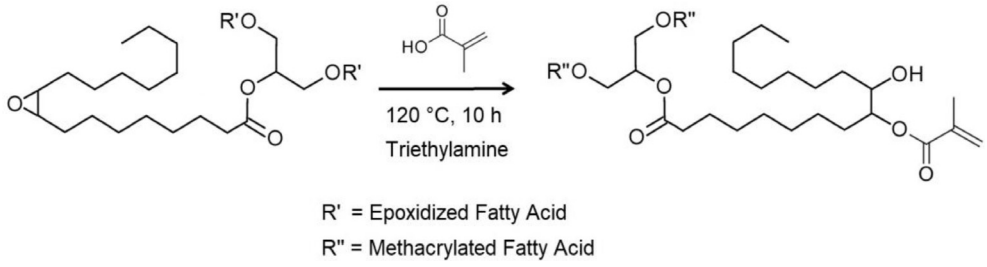

Fig. 1

The synthesis of the methacrylated vegetable oil.

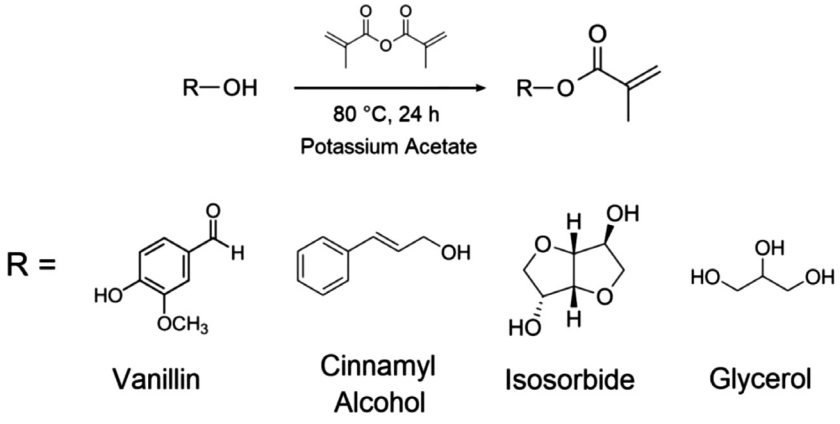

Fig. 2

The synthetic scheme illustrates the production of the bio-based reactive diluents.

After the reaction, the product mixture was cooled and purified. The process involved adding ethyl acetate, an organic diluent, to prevent the modified oil from emulsifying (1:1 by volume). The diluted mixture was quenched with a sodium hydroxide solution (neutralizing the excess methacrylic acid) and washed with distilled water four times to separate the formed sodium methacrylate and catalyst. Lastly, the assisting ethyl acetate was distilled. The pure methacrylated vegetable oil was characterized by ^{1}H NMR and FT-IR.

Methacrylated Oil

^{1}H NMR of methacrylated oil (Fig. S1) (500 MHz, $CDCl_3$) δ 6.12 (d, J = 1.5 Hz, 2H), 5.59 (q, J = 2.1 Hz, 2H), 4.28 (dd, J = 11.9, 4.3 Hz, 2H), 4.17 – 4.07 (m, 3H), 2.31 (tt, J = 7.6, 2.4 Hz, 6H), 2.17 – 1.88 (m, 12H), 1.75 – 1.11 (m, 78H), 0.90 (tt, J = 7.1, 1.6 Hz, 9H).

2.4 Synthesis of the bio-based reactive diluents

The synthesis illustrated in Fig. 2 involved the particular reaction starting alcohol containing free modifiable hydroxyl groups, methacrylic anhydride as a reactive nucleophile, and the reaction catalyst (potassium acetate). The specific reaction mixtures are summarized in Table 1. Each reaction was performed in a 1000 mL round-bottom flask and homogenized using a magnetic stirrer. The reaction conditions were 80 °C and 24 h. After the reaction, the formed methacrylic acid (secondary product) was removed by neutralization with a sodium hydroxide solution. After reaching neutral pH, the accumulated sodium methacrylate, together with the catalyst, was quenched from the mixture with distilled water four times. Lastly, the residual emulsified water was separated over the anhydrous sodium sulfate. The pure, clear, and dry products were analyzed by ^{1}H NMR and FT-IR.

^{1}H NMR of VMA (Fig. S2) (500 MHz, $CDCl_3$) δ: 9.94 (s, 1H), 7.51 – 7.43 (m, 2H), 7.28 – 7.20 (m, 1H), 6.37 (p, J = 1.0 Hz, 1H), 5.78 (p, J = 1.5 Hz, 1H), 3.88 (s, 3H), 2.06 (dd, J = 1.6, 1.0 Hz, 3H).

^{1}H NMR of CMA (Fig. S3) (500 MHz, $CDCl_3$) δ: 7.43 – 7.36 (m, 2H), 7.36 – 7.29 (m, 2H), 7.33 – 7.23 (m, 1H), 6.68 (dt, J = 15.8, 1.5 Hz, 1H), 6.33 (dt, J = 15.9, 6.4 Hz, 1H), 6.16 (dq, J = 2.0, 1.0 Hz, 1H), 5.59 (p, J = 1.6 Hz, 1H), 4.82 (dd, J = 6.3, 1.4 Hz, 2H), 1.98 (dd, J = 1.6, 1.0 Hz, 3H), 1.61 – 1.53 (m, 1H).

^{1}H NMR of IDMA (Fig. S4) (500 MHz, $CDCl_3$) δ 6.10 (q, J = 1.1 Hz, 1H), 6.04 (q, J = 1.1 Hz, 1H), 5.54 (dp, J = 11.7, 1.6 Hz, 2H), 5.20 (dt, J = 2.9, 1.2 Hz, 1H), 5.14 (q, J = 5.5 Hz, 1H), 4.84 (t, J = 5.1 Hz, 1H), 4.47 (d, J = 4.7 Hz, 1H), 3.99 – 3.91 (m, 2H), 3.93 – 3.87 (m, 1H), 3.82 (dd, J = 9.9, 5.2 Hz, 1H), 1.88 (dt, J = 20.0, 1.3 Hz, 6H).

^{1}H NMR of GMA (Fig, S5) (500 MHz, $CDCl_3$) δ 6.15 (q, J = 1.2 Hz, 1H), 5.65 – 5.57 (m, 1H), 4.36 – 4.15 (m, 2H), 4.15 – 3.75 (m, 1H), 3.72 – 3.44 (m, 2H), 1.96 (t, J = 1.3 Hz, 3H).

^{1}H NMR of GTMA (Fig. S6) (500 MHz, $CDCl_3$) δ 6.17 – 6.05 (m, 3H), 5.61 (dtd, J = 10.0, 3.2, 1.6 Hz, 3H), 5.44 (tt, J = 6.0, 4.4 Hz, 1H), 4.46 – 4.15 (m, 4H), 1.95 (dt, J = 12.7, 1.4 Hz, 9H).

2.5 Reactivity study

Differential scanning calorimetry (DSC) was used to investigate the curability of the synthesized systems and molecules. The samples were mixed with Luperox DI and *tert*–butyl peroxide as the thermoinitiator (at a 1 % w/w loading relative to the precursor)

Table 1

The composition of the reaction mixtures formulated to synthesize the bio-based reactive diluents.

Compound	Alcohol (g)	MAAH (g)	Catalyst KAc (g)	Bio-based content (wt. %)
Vanillin Methacrylate (VMA)	152	154	3.0	69.1
Cinnamyl Methacrylate (CMA)	134	154	2.9	66.3
Isosorbide Dimethacrylate (IDMA)	146	308	4.5	51.8
Glycerol Methacrylate (GMA)	92	154	2.5	57.5
Glycerol Trimethacrylate (GTMA)	92	462	5.5	31.1

and placed in aluminum pans (10–15 mg, hermetically sealed). The measurements were conducted using a DSC 2500 from TA Instruments (New Castle, DE, USA). Four heating scans were performed on each sample from 30 to 200 °C, with temperature ramps of 5, 10, 15, and 20 °C/min. The obtained results were used to calculate the kinetics parameters from Kissinger's theory.

2.6 Rheological investigation

Firstly, the curable multi-component systems were formulated from the methacrylated oil and the reactive diluents. Also, the photoinitiator (1 wt. %) was added to each reactive system. The rheological study was conducted to describe the diluting effect of the bio-based enhancing additives mixed with the high-viscosity methacrylated oil. We used the TA Instruments rheometer AR-G2 for the investigation. The prepared systems were measured under the following conditions: 500 µL of sample, the Peltier platform and cone-plate geometry (40 mm, 2° angle), a shear rate of 10 s^{-1}, and a temperature ramp from 25 to60 °C. The obtained results were used to calculate flow-kinetics parameters from the Arrhenius law.

2.7 Thermal stability

The tested photo-cured specimens were fabricated by MSLA 3D printing. We used a PRUSA SL1S SPEED 3D printer (Prusa Research Ltd., Czech Republic). The print settings were as follows: the first layer's exposure time was 40 s, and all subsequent layers' exposure time was 15 s. The set layer thickness was 50 µm. The cured specimens were cleaned with isopropanol and post-cured under a 405 nm LED light for one hour. Thermo-gravimetric analysis (TGA) determined the thermal stability of the cured thermoset. We used the TGA Q500 from TA Instruments (New Castle, DE, USA). The degradation of a sample (10–15 mg) was monitored using the following heating program: equilibration at 40 °C; heating to 600 °C at 10 °C/min under N_2; 10 min at 600 °C under an air atmosphere. The obtained results were used to calculate the heat-resistance index, which served as a comparable parameter.

2.8 Mechanical performance

The performed flexural mechanical tests involved the standard rectangular specimens with dimensions of 80 × 10 × 4 mm fabricated by MSLA 3D printing. The printed specimens were cured after the 3D printing for 30 min by a 405 nm irradiation source, exposing 8 mW·cm^{-3} emission power. The flexural test was conducted in accordance with CSN EN ISO 178. The loading nose and support radius were 5 mm, and the support span was 64 mm. The test speed was set to 10 mm·min^{-1}. Each investigated photo-cured system was measured at least five times, and the appropriate statistical parameters were included in the summarized results. We performed the gel content measurements according to the norm ASTM D2765–16. The sample was extracted from the Soxhlet extractor, dried until constant weight, and then the gel content was calculated according to the following Eq. (1) [38]:

$$Gel\ Content = \frac{w_1}{w_2} * 100\%, \quad (1)$$

where w_1 (g) is the weight of the sample after the test, and w_2 (g) stands for the weight of the sample before the test.

3 Results and discussion

3.1 Synthesis and structural characterization

The modified vegetable oil was synthesized from commercially available epoxidized oil via a nucleophilic substitution mechanism catalyzed by the organic base, triethylamine. The base-involving catalysis is essential for the oxirane "ring opening" reaction, as it increases the nucleophilic character of methacrylic acid. The amine salt of the reacting carboxylic acid comprises two ions – a carboxylate anion with cumulated negative charge (strong nucleophile character) on the deprotonated carboxyl functional group, and an amine cation which increases the nucleophilic character of the acid, and provides the hydrogen ion to protonate the "ring opened" oxygen atom [39,40]. This reaction, leading to the modified vegetable oils, was previously investigated; however, we used less toxic and volatile methacrylic acid compared to the commonly used acrylic acid, published in numerous available articles and investigations (66–68 % yield of acrylated oil, [41] or 49 % yield of the acrylated product [42]). Regarding the structural verification of the synthesized methacrylated vegetable oil, the ^1H NMR spectrum shown in Fig. S25 reveals methylidene signals between 6.25 and 5.5 ppm. These signals confirm the presence of methacrylate functional groups [43]. This chemical structure change is also evident from FTIR spectra (see Fig. S7), where the methylidene group confirms two separate signals –$C = C$ stretching 1662–1626 cm^{-1}

Table 2

The summarized names, structures, and achieved yields of the synthesized reactive systems.

Compound	Structure	Yield
Methacrylated Oil	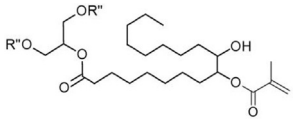	94.5 %
Vanillin Methacrylate (VMA)	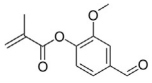	88.9 %
Cinnamyl Methacrylate (CMA)	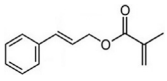	91.2 %
Isosorbide Dimethacrylate (IDMA)	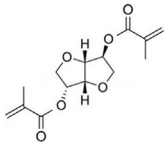	85.4 %
Glycerol Methacrylate (GMA)	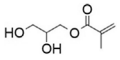	72.2 %
Glycerol Trimethacrylate (GTMA)	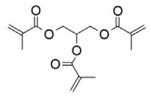	92.1 %

and C–O (ester) stretching 1210–1163 cm^{-1}. Additionally, the "ring opening" nucleophilic substitution is confirmed by the occurring O–H stretching signal at a wavelength interval of 3550–3200 cm^{-1}. All the reactive diluents synthesized in this work achieved high yields (see Table 2), and their production involved a much more sustainable catalyst than in previously published works. The similar methacrylic anhydride-involving methacrylate reactions available in the literature reached product yields of 58.3 % [44] or 50–80 % [45]. Moreover, the majority of MAAH-involved methacrylate reactions were catalyzed by 4-dimethylaminopyridine (DMAP) [44–46], which is an expensive and hazardous catalyst compared to the proposed potassium acetate. The lowest yield of 72.2 % was achieved for glycerol methacrylate (GMA) due to its high water solubility, attributed to two vacant hydroxyl groups. The purities of all synthesized products were verified via NMR analysis combined with acidity measurements, since all the produced compounds were purified via the neutralization of the formed methacrylic acid. The residual acidity was eliminated above 99 % for all synthesized products (measured acidity values reached <1 mg KOH/g).

3.2 Reactivity investigation and evaluation

The polymerization activity of the methacrylate functional groups in the methacrylated oil and the structures of the synthesized reactive diluents are crucial factors that directly determine the tendency towards curing and serve as comparison parameters. Generally, the increasing molecular weight of the precursor leads to higher reactivity values. The large molecular structure of the molecule complicates ongoing radical polymerization by reducing molecular mobility due to steric factors [47,48]. Also, the higher functionality leads to the rise of the polymerization parameters due to the combination of the factors. Molecules with two or more curable functional groups must be initiated multiple times compared to mono-functional molecules. Moreover, the highly crosslinked molecular sites formed by multi-functional precursors exhibit a rigid/impenetrable structure, preventing the additional radicals from being efficiently transported [49,50]. The particular reactivity parameters were calculated from Kissinger's theory, which has been numerously interpreted in the literature [47–50]. The mathematical equation stands as follows (2):

$$\ln\left(\frac{\beta}{T_p^2}\right) = \ln\left(\frac{AR}{E_a}\right) - \frac{E_a}{R}\cdot\frac{1}{T_p}, \tag{2}$$

where β is the heating rate (°C/min); T_p is the exothermic peak temperature (°C); A is the pre-exponential factor (-); E_a is activation energy of the reaction (J/mol) and R is the gas constant (J/(mol·K)). The activation energy generally describes the system's tendency to polymerize. The summarized DSC results shown in Fig. 3 indicate that the methacrylated vegetable oil exhibited the highest activation energy (162.8 kJ/mol). This result is supported by the oil's high molecular weight (above 1000 g/mol) and its multiple functionality (the average methacrylate functional group number per molecule is above 2.5, as determined by NMR analysis). Similar results were reported for the analogous compounds [51]. As discussed earlier, the multi-functional precursors reached the higher activation energies – IDMA achieved E_a of 119.4 kJ/mol, and GTMA exhibited E_a of 149.2 kJ/mol. On the other hand, the mono-functional molecules (VMA, CMA, and GMA) had the lowest activation energies. Due to the low molecular weight and free hydroxyl groups, GMA

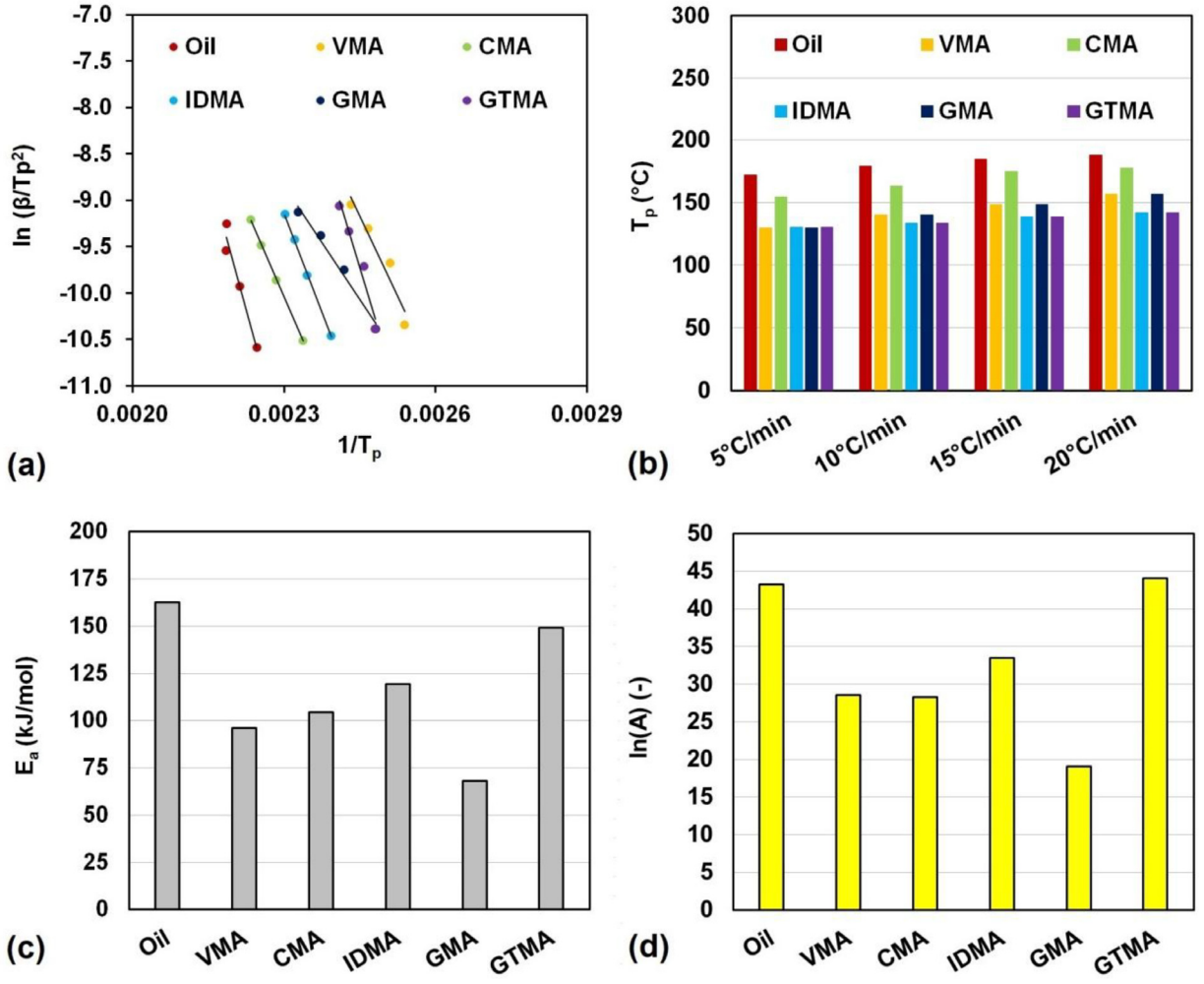

Fig. 3

The reactivity investigation results obtained by DSC measurements. (a) The graphical interpretation of Kissinger's theory, (b) The peak temperatures recorded for each curable system, (c) The calculated activation energy values (E_a), (d) The calculated pre-exponential factor values (ln(A)).

reached the lowest E_a of 68.2 kJ/mol. Polar functional groups, such as hydroxyl, amine, and carbonyl groups, lower the activation energy [52]. The pre-exponential factor (ln(A)) generally describes the reaction's tendency to proceed further [53]. The calculated values show a trend similar to that of the activation energies.

3.3 System formulations and rheological study

The synthesized reactive diluents were mixed with the high-viscosity methacrylated oil to demonstrate modifications in flow properties and enhancement in thermal/mechanical properties. The eventual composition of the prepared curable liquid precursors is illustrated in Fig. 4. The enhancement of the methacrylated vegetable oil was investigated due to the excessive rheological profile and poor mechanical performance of modified oil-based resins reported in the published literature [54,55]. Firstly, the rheological behavior was investigated before the photo-curing. Since photo-curability should be confirmed by MSLA 3D printing, the apparent viscosity is a key parameter given stereolithography's hardware limitations [56]. The comparison parameters for the rheological characterization were calculated for the Arrhenius law. The used mathematical equation stands as follows (3): [35]

$$\ln \eta = \frac{E_\eta}{R} \cdot \frac{1}{T} + \ln \eta_\infty, \tag{3}$$

where the dependence of apparent viscosity ln (η) (-) on the reverse value of temperature 1/T (K^{-1}) is constructed, E_η is the flow activation energy (J/mol), R stands for the universal gas constant R (J/(mol·K)), and η_∞ represents the infinite-temperature viscosity (Pa·s). The determined flow curves of the prepared photo-curable mixtures, together with the calculated parameters from the Arrhenius plot, are displayed in Fig. 5.

As shown by the rheological measurements, the initiated apparent viscosity of the methacrylated oil is approximately 4000 mPa·s at 25 °C. According to the literature, the limit apparent viscosity for 3D printing is approximately 5000 mPa·s [56]. Although the pure methacrylated oil should be printable, the potentially improved fluidity of the system is a positive factor. The best diluting properties were exhibited by CMA, providing the apparent viscosity of 405 mPa·s at 25 °C. The strongly non-polar compounds exhibiting multiple functionality, GTMA and IDMA, performed as effective diluents

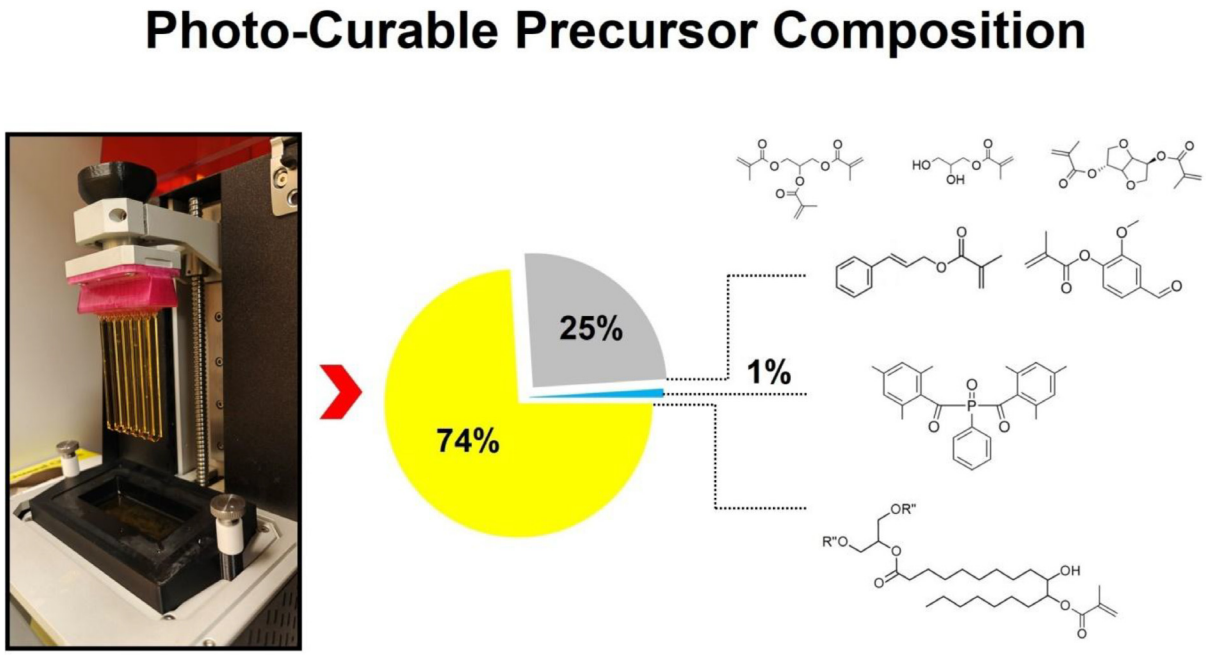

Fig. 4

The photo-curable resin weight composition comprises mainly methacrylated oil (74 %), supplemented with synthesized diluents (25 %) and homogenized with the photoinitiator BAPO (1 %).

(GTMA-involved precursor reached 747 mPa·s at 25 °C and IDMA-involved precursor achieved 1323 mPa·s at 25 °C). The least diluting molecules, VMA and GMA, provide minor flow modification. VMA's apparent viscosity is higher due to the presence of a carbonyl functional group, which provides Keesom molecular interactions and serves as an H-bonding acceptor. GMA's structure contains two free hydroxyl groups, which form H-bonds with each other and with the electronegative atoms in the methacrylated oil. The flow activation energies practically correspond with the observable rheological curves. The VMA- and GMA-involved reached opposite flow activation energies relative to the measured viscosity at 25 °C (VMA's E_η reached 58.5 kJ/mol, GMA's E_η reached 51.5 kJ/mol). This outcome is likely caused by the continuous decrease in GMA's viscosity with increasing temperature, due to its lower molecular weight and more complex molecular interactions at elevated temperatures [30]. Each synthesized compound contributed to a decrease in viscosity, which positively affected MSLA 3D printing for photo-cured fabrication of specimens.

3.4 Photo-curing study

We used FT-IR to provide additional curing characteristics to Kissinger's theory, which was performed earlier in the investigation in subSection 3.2. The thermal DSC connected to the theoretical calculation of the reactivity parameters is often used in literature to provide a detailed description of the selective reactive compounds and molecules used for both thermal- and photo-curing purposes [49,57]. While Kissinger's theory provides the calculated thermodynamic parameters and values, the photo-curing SLA 3D application especially demands particular conditions from the photo-irradiation standpoint. The exposure power, irradiation source wavelength, and the exposure duration are critical factors for stereolithography [58]. The FI-TR instrumentation analyzed the decreasing signals of the methylidene polymerizable groups; therefore, it can provide information regarding the curable double bond conversions. The calculation of the double bond conversion was performed according to Eq. (4) [59]:

$$Double\ Bond\ Conversion = \left(1 - \frac{\left(\frac{A_{C=C}}{A_{C=O}}\right)_{cured}}{\left(\frac{A_{C=C}}{A_{C=O}}\right)_{uncured}}\right) \times 100, \quad (4)$$

where the double bond conversion is calculated from $A_{C=C}$ (integral area of methylidene $C = C$ stretching signal) and $A_{C=O}$ (integral area of $C = O$ stretching signal of ester). The photo-curing study using FT-IR is illustrated in Fig. 6.

The double bond conversion results in Fig. 6 (other FT-IR graphs are added to the Supporting information) correspond with the previously obtained characterizations from the thermal DSC investigation and Kissinger's theory values. The pure oil possessed the highest polymerization activation energy, and the FT-IR curing study confirmed that the pure methacrylated oil reached the lowest double conversion rate (achieving double bond conversion of 23.1 % after 10 min and the eventual conversion of 66.7 % after 30 min). The second least reactive compound from the thermal DSC analysis, GTMA, achieved the second lowest double bond conversion after 10 min (68.9 %). On the other hand, the most reactive diluent, GMA, achieved the highest double bond conversion rate (see graphs in Fig. 6), when the double bond conversion reached 92.1 % and remained constant after 30 and 120 min of curing. The rest of the reactive diluents showed the continuous decrease of the reactivity in the same

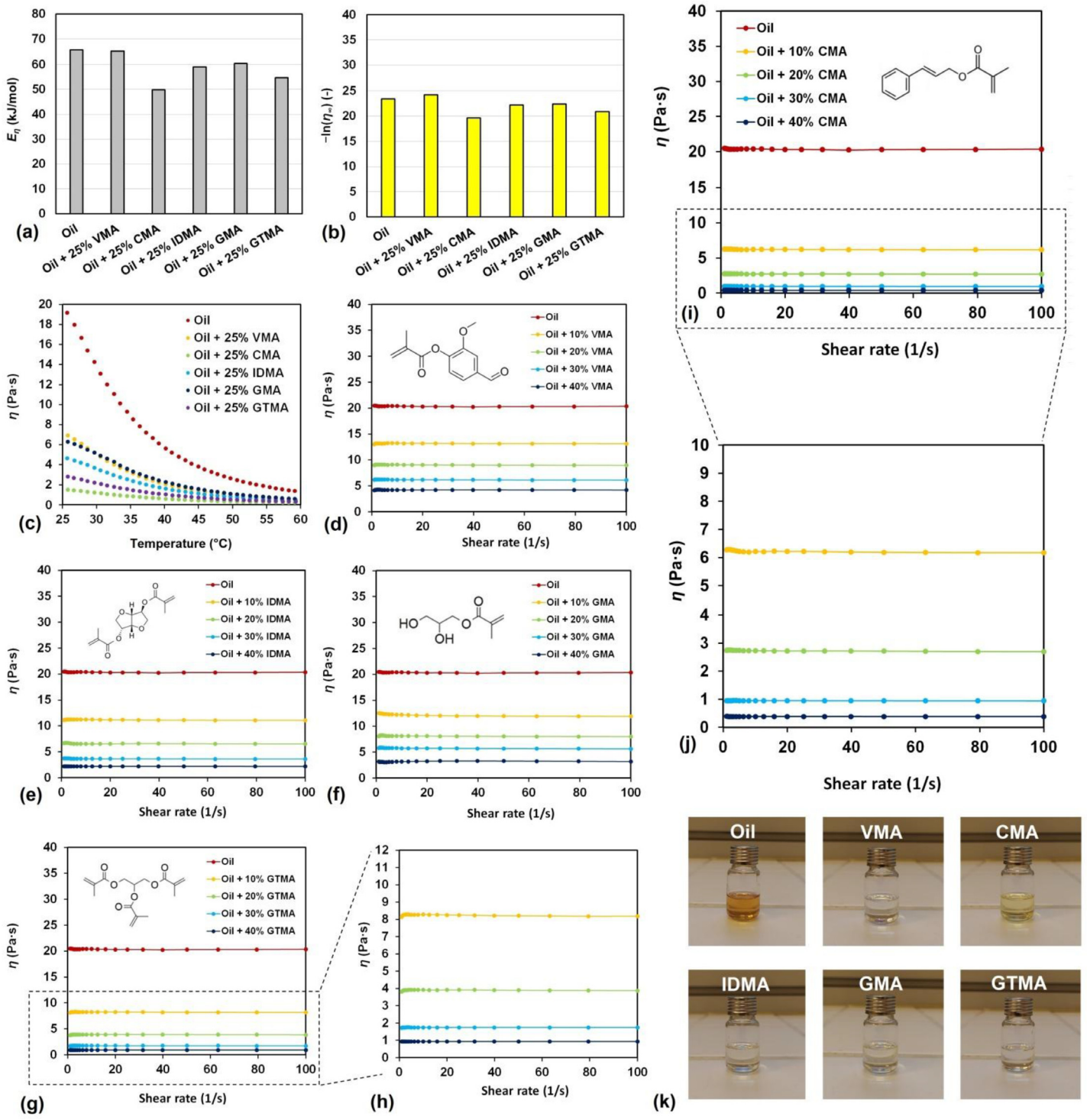

Fig. 5

Rheological study of the prepared photo-curable systems. (a) The calculated flow activation energies from the Arrhenius law. (b) The calculated pre-exponential factors (infinite-temperature viscosities) from the Arrhenius law. (c) The dependence of the apparent viscosity on the temperature of the studied photo-curable systems. (d) The rheological investigation of the diluting effect of Vanillin Methacrylate (VMA). (e) The rheological investigation of the diluting effect of Isosorbide Dimethacrylate (IDMA). (f) The rheological investigation of the diluting effect of Glycerol Methacrylate (GMA). (g,h) The rheological investigation of the diluting effect of Glycerol Trimethacrylate (GTMA). (i,j) The rheological investigation of the diluting effect of Cinnamyl Methacrylate (CMA). (k) The photos of the synthesized compounds.

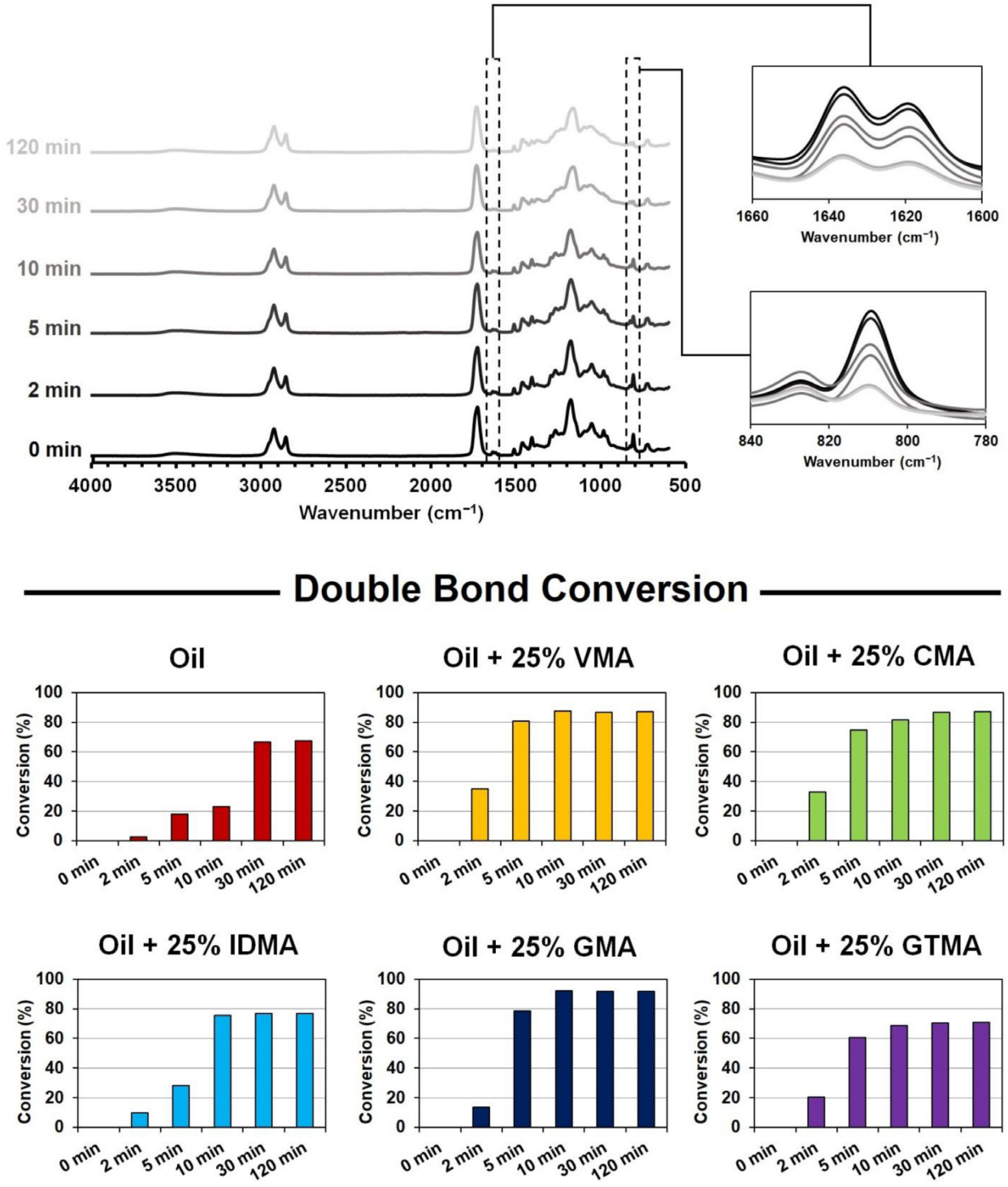

Fig. 6

The photo-curability study (the pure methacrylated oil illustrated) provided by FT-IR analysis during the irradiation exposure of the formulated curable oil-based systems with different reactive diluents.

order as Kissinger's theory calculated: VMA (conversion after 10 min 88.7 %), CMA (conversion after 10 min 81.6 %), and IDMA (conversion after 10 min 75.7 %). The combined results of Kissinger's theory calculation and the FT-IR-provided photo-curing study confirmed that the presence of polar functional groups (hydroxyl from GMA and carbonyl/alkoxy from VMA) increases the reactivity of the curable system. The functionality of the reactive diluent also plays a major role (the most reactive GMA contains one polymerizable group, while GTMA possesses three methylidene groups). The similar effects of the polar functional groups on the photo-curability and the functionality of the cured systems were observed in the published literature [30,60,61]. This

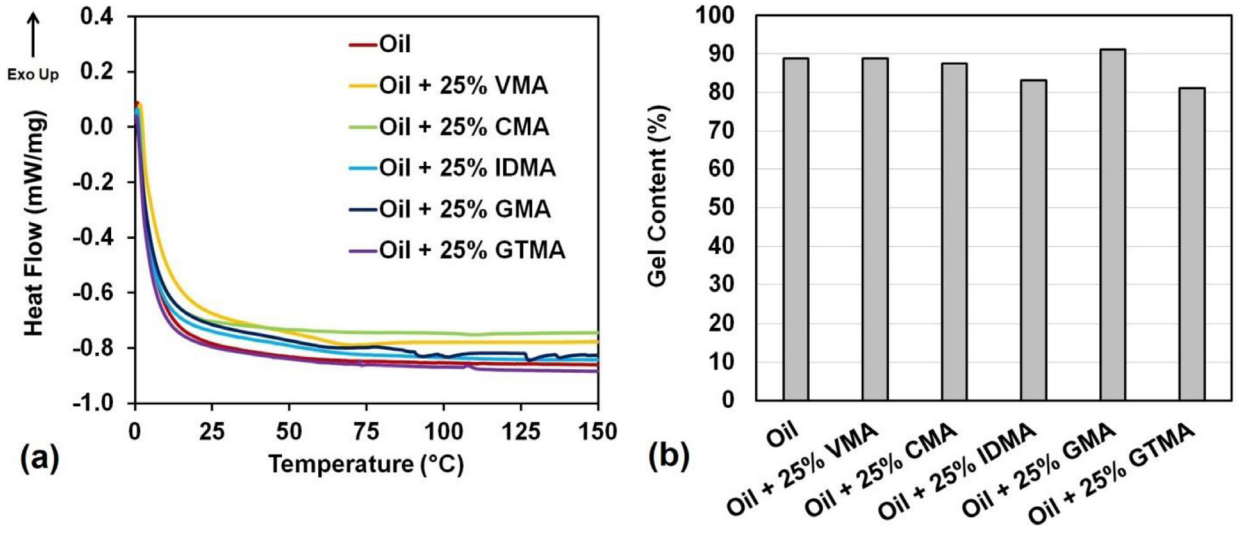

Fig. 7

(a) The post-curing DSC study uncovers the total polymerization of the photo-curable prepared systems. (b) The gel content achieved by the photo-cured formulated systems.

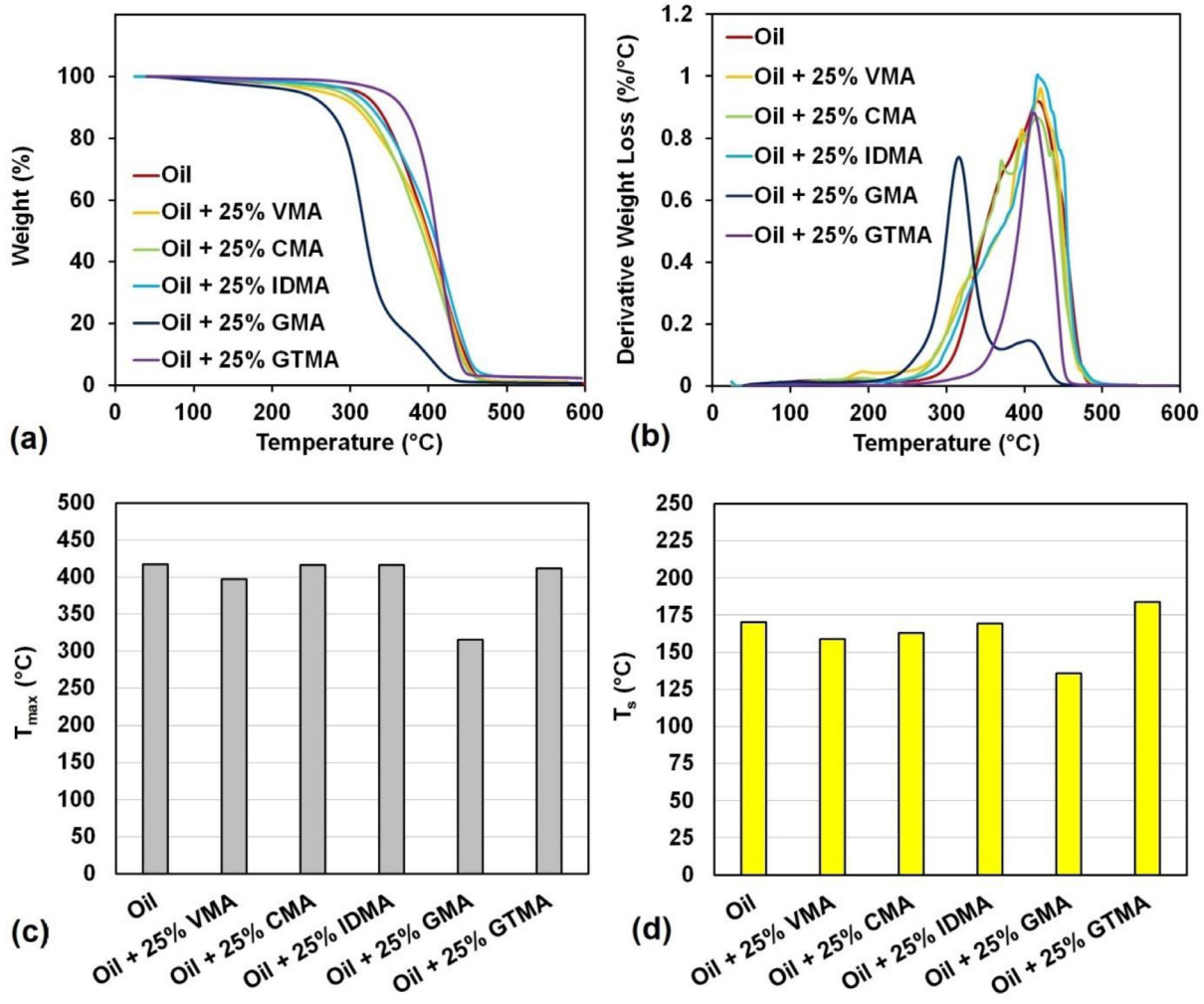

Fig. 8

The thermal stability investigation was conducted using the TGA measurements. (a) The measured TGA degradation curves, (b) The derivative weight loss dependence on the temperature obtained from TGA, (c) The determined inflection points marking the maximal rate of mass change (T_{max}), (d) The calculated heat-resistant indexes (T_s).

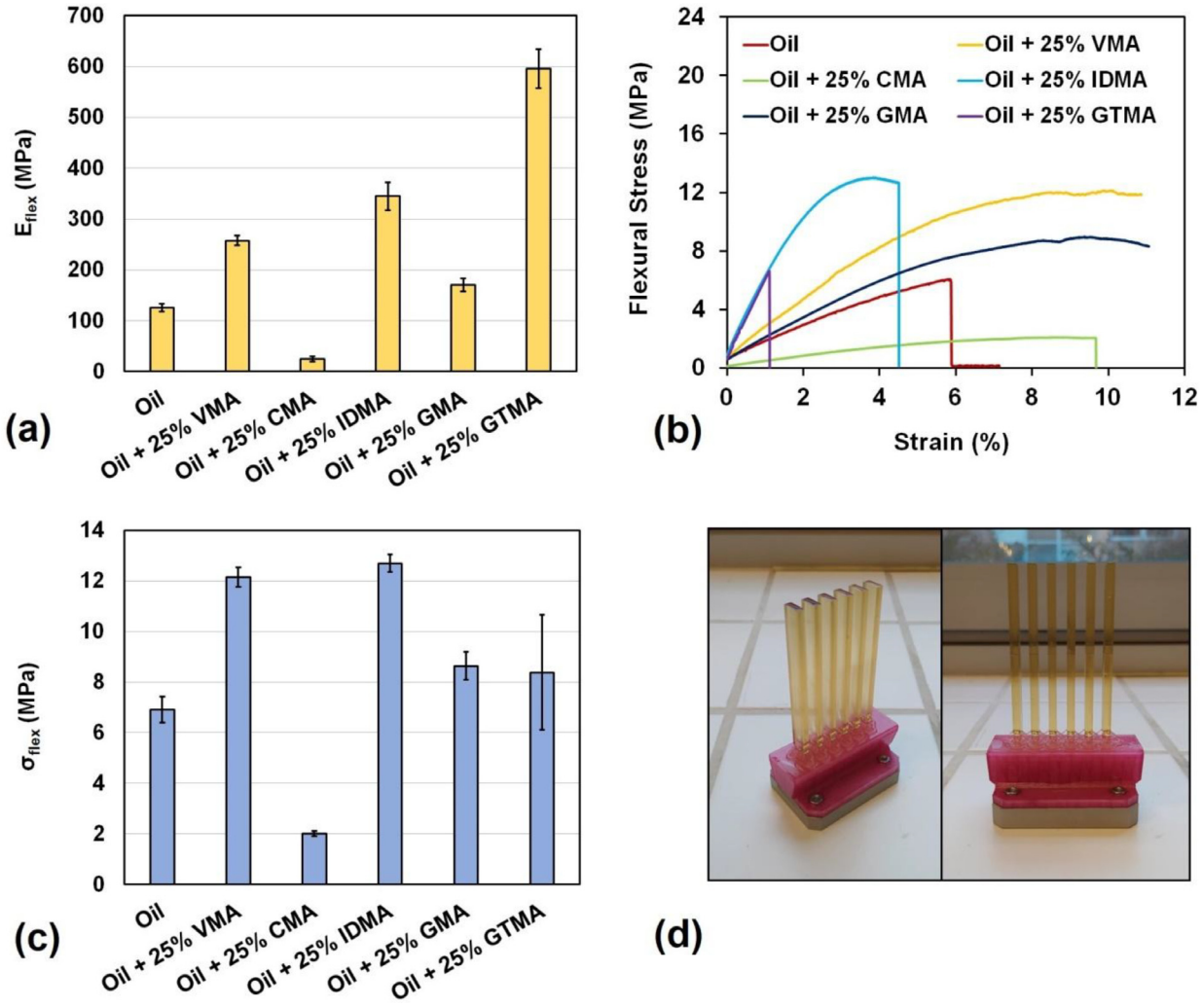

Fig. 9

The mechanical properties determined from the flexural tests. (a) The measured flexural modulus (E_{flex}) of the photo-cured resins, (b) The overlay stress-strain curves selected for all the investigated photo-cured resins, (c) The measured flexural strengths (σ_{flex}) of the photo-cured resins, (d) The real photo of the fabricated specimens produced by MSLA 3D printing.

investigation uncovers an important factor influencing the SLA 3D printing strategies focused on the potentially faster-curing systems involving functional groups with polar character, such as GMA or VMA.

3.5 Thermal stability and mechanical performance

The photo-cured resins were studied from a thermal stability standpoint to describe the effect of added reactive diluents on the commonly thermally stable molecular sites of the polymerized triacylglycerides. The performed DSC analysis (see Fig. 7) confirmed the total polymerization of the photo-cured systems, as no exothermic heat release was detected. Fig. 7 also contains results from the gel content determined for the photo-cured systems. As conducted investigations have shown, the ester bond between glycerol and fatty acids is relatively thermodynamically stable compared to other ester bonds, such as those in methacrylate or acrylate groups [62]. We applied the heat-resistance index calculation to incorporate a quantitative parameter into the potential literature comparison, given its common use in published papers on the investigation of the modified curable oil [63,64]. The used mathematical equation referring to the heat-resistant index (T_s) stands as follows (5): [63]

$$T_s = 0.49[T_5 + 0.6(T_{30} - T_5)], \quad (5)$$

where T_s is the heat-resistant index (°C); T_5 stands for the temperature at 5 % of mass loss (°C), and T_{30} stands for the temperature at 30 % of mass loss (°C). As shown in Fig. 8, the inflection points (T_{max}), marking the maximum rate of mass change, are practically identical for all cured oil-based systems with reactive diluents, except for VMA- and GMA-based thermosets. The VMA-involving system reached T_{max} slightly below 400 °C, likely due to the thermally unstable carbonyl group, which may contribute to the thermal instability [65]. The lowest thermal stability was exhibited by the GMA-involving thermoset, reaching T_{max} of 316 °C and T_s of 136 °C, likely due to the highly thermally unstable free hydroxyl groups [66]. On the other

hand, the GTMA-involving photo-cured thermoset reached the best thermal stability, which is evident from the TGA degradation curve (Fig. 8(a)), from the reached T_{max} (412 °C) value, and also confirmed by the calculated T_s of 184 °C. The high crosslinking provided by the three-functional GTMA significantly enhanced the overall thermal stability. This effect, provided by the highly functionalized crosslinker, has been reported in the literature [67]. The remaining reactive diluents, CMA and IDMA, exhibited thermal stability that was practically equivalent to that of the pure methacrylated oil.

The mechanical performance was demonstrated through standard flexural tests, summarized in Fig. 9. The entering flexural parameters of the pure cured methacrylated oil involve the flexural modulus of 126 ± 8 MPa and the flexural strength of 6.9 ± 0.5 MPa. These determined parameters correspond to published similar cured thermosets [68,69]. The mechanical enhancement was not confirmed for the CMA-involving photo-cured resin. This investigated system exhibited a much lower flexural modulus (25 ± 5 MPa) and the flexural strength (2.0 ± 0.1 MPa) than the pure cured methacrylated oil. Since CMA is a mono-functional curable molecule with a relatively long carbon backbone, the mechanical properties are significantly decreased. Regarding the flexural modules, the GMA-involving system achieved results similar to those of the pure oil (E_{flex} of 170 ± 13 MPa). VMA-involving system reached an increased modulus of 105 %, IDMA enhanced the increase of 174 %, and the best-performing highly crosslinked GTMA-involving systems achieved the rise of 373 %. The flexural strengths were improved in all the prepared photo-cured thermosets except for the CMA-involving system. The highest flexural strengths were reached by the IDMA-involving system (σ_{flex} of 12.7 ± 0.3 MPa) and the VMA-involving resin (σ_{flex} of 12.1 ± 0.4 MPa). When both parameters were combined, the IDMA-involved system exhibited the most significant mechanical enhancement in terms of rigidity/hardness. The flexibility enhancement was notable in the VMA-involving system, with a substantial increase in the limit strain of above 80 % (while the specimens remained undamaged, as shown in Fig. 9(b)). The rigid character of the IDMA-involving system is likely due to the di-functional IDMA's crosslinking nature. On the other hand, the mono-functional VMA, containing polar and H-bond-accepting functional groups (carbonyl, ester, and methoxy), exhibited the best flexural-enhancing effect.

4 Conclusions

This investigation article focuses on a comprehensive comparison of the enhancing effects of selected bio-based curable low-molecular additives on a curable oil-based photo-curable resin processed by MSLA 3D printing. The work involves the synthesis of the main curable high-viscosity systems, methacrylated vegetable oil, and also the chemical production of five different polymerizable compounds from renewable sources – vanillin methacrylate (VMA), cinnamyl methacrylate (CMA), isosorbide dimethacrylate (IDMA), glycerol methacrylate (GMA), and glycerol trimethacrylate (GTMA). All the synthesized structures were analyzed by NMR and FTIR, achieving yields over 85 %, except for GMA, which yielded 72.2 %. The syntheses of CMA and GTMA were the most efficient because of the optimal viscosities of the products. Then, the reactivity and overall polymerization activity were investigated using Kissinger's theory. GMA proved to be the best reactivity enhancer, achieving an activation energy of 68.2 kJ/mol. The polar, free hydroxyl groups enhanced GMA's reactivity. Subsequently, the multi-component curable mixtures were formulated of the methacylated vegetable oil, a reactive diluent, and a photoinitiator. The rheological investigation revealed that the CMA-involving system exhibited the lowest measured viscosity (405 mPa·s at 25 °C) and the lowest Arrhenius flow-kinetics parameters. The thermal stability study using TGA measurements revealed that GMA significantly decreased the calculated heat-resistant index (T_s dropped from 170 °C to 135 °C). On the other hand, GTMA enhanced thermal stability, and the GTMA-containing system achieved a T_s of 184 °C. Eventually, the mechanical investigation, provided by the standard flexural tests, revealed the highest flexural modulus for the GTMA-involving system (596 ± 38 MPa). The highest flexural strength was achieved by IDMA-involving resin (12.7 ± 0.3 MPa). CMA failed to enhance the mechanical properties fully. The investigation uncovered that IDMA is an ideal bio-based enhancer for rigid methacrylated oil-based thermosets, while VMA significantly enhances the potential of flexible, highly bio-based photo-cured resins.

Supporting information

The supporting file contains NMR spectra (Figs. S1-S6), FTIR spectra (Figs. S7-S12), DSC data (Figs. S13-S18), the flexural stress-strain curves (Figs. S19-S24), the summarized NMR data (Fig. S25), and the FT-IR photo-curing investigation (Figs. S26-S30).

Declaration of competing interest

The authors declare that they have no known competing financial interests or personal relationships that could have appeared to influence the work reported in this paper.

Data availability

Data will be made available on request.

CRediT authorship contribution statement

Vojtěch Jašek: Writing – review & editing, Writing – original draft, Visualization, Methodology, Investigation, Formal analysis, Data curation, Conceptualization. **Otakar Bartoš:** Methodology, Formal analysis. **Jan Prokeš:** Methodology, Formal analysis. **Silvestr Figalla:** Validation, Supervision. **Radek Přikryl:** Validation, Supervision.

Acknowledgements

V.J. acknowledges the financial support from the Ministry of Education, Youth and Sport of the Czech Republic (project No FCH-S-26-9028).

Supplementary materials

Supplementary material associated with this article can be found, in the online version, at doi:10.1016/j.giant.2026.100391.

References

[1] Mary Anne S. Melo, Isadora Martini García, L. Mokeem, Michael D. Weir, Hockin H.K. Xu, C. Montoya, S. Orrego, Developing bioactive dental resins for restorative dentistry, J. Dent. Res. 102 (11) (2023) 1180–1190, doi:10.1177/00220345231182357.

[2] L. Papadopoulos, L. Pezzana, Natalia Maria Malitowski, N. Kladovasilakis, D. Tzetzis, M. Sangermano, Dimitrios N. Bikiaris, T. Robert, Itaconic acid-based 3D printed nanocomposites: an In-depth study on the effect of nanoinclusions on the physicochemical properties and the printability of formulations based on polyester itaconates, Giant 18 (2024) 100275-100275, doi:10.1016/j.giant.2024.100275.

[3] N. Zhang, Z. Wang, Z. Zhao, D. Zhang, J. Feng, L. Yu, Z. Lin, Q. Guo, J. Huang, J. Mao, J. Yang, 3D Printing of micro-nano devices and their applications, Microsyst. Nanoeng. 11 (1) (2025) 35, doi:10.1038/s41378-024-00812-3.

[4] S. Salifu, D. Desai, O. Ogunbiyi, K. Mwale, Recent development In the additive manufacturing of polymer-based composites for automotive structures—A review, Int. J. Adv. Manuf. Technol. 119 (11–12) (2022) 6877–6891, doi:10.1007/s00170-021-08569-z.

[5] T. Aziz, F. Haq, A. Farid, C. Li, Lai Fatt Chuah, A. Bokhari, M. Mubashir, Doris Ying Ying Tang, Pau Loke Show, The epoxy resin system: function and role of curing agents, Carbon lett. 34 (1) (2023) 477–494, doi:10.1007/s42823-023-00547-7.

[6] Md.Mostafizur Rahman, M.A. Islam, Application of epoxy resins In building materials: progress and prospects, Polym. Bull. 79 (3) (2021) 1949–1975, doi:10.1007/s00289-021-03577-1.

[7] R. Mori, Replacing all petroleum-based chemical products with natural biomass-based chemical products: a tutorial review, RSC Sustain. 1 (2) (2023) 179–212, doi:10.1039/d2su00014h.

[8] G. Pitzanti, V. Mohylyuk, F. Corduas, Niall M. Byrne, Jonathan A. Coulter, Dimitrios A. Lamprou, Urethane dimethacrylate-based photopolymerizable resins for stereolithography 3D printing: a physicochemical characterisation and biocompatibility evaluation, Drug Deliv. Transl. Res. 14 (1) (2023) 177–190, doi:10.1007/s13346-023-01391-y.

[9] S. Cho, Young Soo Lee, S. Choi, Y. Chae, S.-M. Park, S.-kyun Ahn, M. Seo, Impact-resistant, haze-free, 3D-printable transparent block copolymer resin via photopolymerization-induced microphase separation, NPG Asia Mater. 17 (1) (2025) 37, doi:10.1038/s41427-025-00618-3.

[10] Mohamed A. El-Tayeb, Turki M. Dawoud, Khalid S. Almaary, F. Ameén, Hossein Ali Khonakdar, Synthesis, 3D printing, and characterization of biobased antibacterial scaffolds using acrylated epoxidized soybean oil-Co-hydroxyethyl methacrylate, J. Polym. Env. 33 (1) (2024) 358–373, doi:10.1007/s10924-024-03426-y.

[11] Y. Choi, J. Yoon, J.-Y. Kim, C. Lee, Jae Sang Oh, N. Cho, Development of bisphenol-A-glycidyl-methacrylate- and trimethylolpropane-triacrylate-based stereolithography 3D printing materials, Polym. (Basel) 14 (23) (2022) 5198-5198, doi:10.3390/polym14235198.

[12] M. Liu, G.-M. Li, P. Wang, W.-Y. Ying, Y. Yang, C.-Y. Tang, Y. Li, S. Chen, Mechanically enhanced 3D printable photocurable resin composed of epoxy waste cooking oil and triethylene glycol dimethacrylate, J. Polym. Res. 31 (6) (2024), doi:10.1007/s10965-024-04029-w.

[13] L. Yang, J. Wang, R. Li, Y. Gao, H. Wang, Preparation of uv curable acrylamide modified epoxy resin and performance In 3D printing, React. Funct. Polym. 205 (2024) 106093-106093, doi:10.1016/j.reactfunctpolym.2024.106093.

[14] L. Montaina, R. Carcione, F. Pescosolido, M. Montalto, S. Battistoni, E. Tamburri, Three-dimensional-printed polyethylene glycol diacrylate-polyaniline composites by In situ aniline photopolymerization: an innovative biomaterial for electrocardiogram monitoring systems, ACS Appl. Electron. Mater. 5 (1) (2023) 164–172, doi:10.1021/acsaelm.2c01181.

[15] Ernest Mbamalu Ezeh, Advances In the development of polyester resin composites: a review, World J. Eng. (2024), doi:10.1108/wje-12-2023-0517.

[16] G. Rizzo, S. Dattilo, V. Prasad, M. Yasar, A. Ivankoviç, A. Latteri, G. Cicala, Enhancing sustainability In unsaturated polyester resin: a way to use biobased curing agents for reduced styrene content and improved recyclability properties, ACS Appl. Polym. Mater. 6 (10) (2024) 5714–5725, doi:10.1021/acsapm.4c00388.

[17] Elina L.K. Pakkanen, Tuomo P. Kainulainen, Juha P. Heiskanen, Furfural-based vinyl ester resins: syntheses, properties and comparison to bisphenol A-glycidyl methacrylate-based vinyl ester resin, ACS Appl. Polym. Mater. 7 (15) (2025) 10191–10200, doi:10.1021/acsapm.5c01980.

[18] B. Ali, A. Irshad, M. Atif, Bio-based photo-curable polyurethane composites, Polym. Adv. Technol. 34 (2) (2022) 452–473, doi:10.1002/pat.5909.

[19] Q. Li, Jie Hao Qu, Zi Zhao Qian, H. Sun, Lu Jie Wang, F. Fu, Xiang Dong Liu, Reactive diluent strategy for General Benzoxazine to achieve high performance thermoset via A combination of styrene and glycidyl methacrylate, J. Polym. Sci. 60 (5) (2021) 774–784, doi:10.1002/pol.20210741.

[20] Ainakulova Dana Tulegenkyzy, P.S.M. Megat-Yusoff, Khaldun M. Al Azzam, Bekbayeva Lyazzat Kairatovna, A. Goyal, G. Eshmaiel, E.-S. Negim, E. Kusrini, M. Samy, Tailoring epoxy resin properties using glycidyl methacrylate-based reactive diluents: viscosity reduction and performance enhancemen, Int. J. Technol. 16 (4) (2025) 1421-1421, doi:10.14716/ijtech.v16i4.7687.

[21] C. Wang, A. Singh, Erik G. Rognerud, Robynne E. Murray, Grant M. Musgrave, M. Skala, P. Murdy, Jason S. DesVeaux, S. Nicholson, K. Harris, Richard B. Canty, F. Mohr, Alison J. Shapiro, D. Barnes, R. Beach, Robert D. Allen, Gregg T. Beckham, Nicholas A. Rorrer, Synthesis, characterization, and recycling of bio-derivable polyester covalently adaptable networks for industrial composite applications, Matter 7 (2) (2023) 550–568, doi:10.1016/j.matt.2023.10.033.

[22] M. Maturi, E. Locatelli, Alberto Sanz de León, Mauro Comes Franchini, Sergio I. Molina, Sustainable approaches In vat photopolymerization: advancements, limitations, and future opportunities, Green Chem. 27 (29) (2025) 8710–8754, doi:10.1039/d5gc02299a.

[23] J.-Y. Lee, S.-E. Lee, D.-W. Lee, Current status and future prospects of biological routes to bio-based products using raw materials, wastes, and residues As renewable resources, Crit. Rev. Env. Sci. Technol. 52 (14) (2021) 2453–2509, doi:10.1080/10643389.2021.1880259.

[24] Xia, L.; Gui, T.; Wang, J.; Tian, H.; Wang, Y.; Ning, L.; Wu, L. Bio-based coatings: progress, challenges and future perspectives. *Polymers* 2025, 17 (24), 3266–3266. https://doi.org/10.3390/polym17243266.

[25] Vinoth Kumar Selvaraj, J. Subramanian, I. Suyambulingam, S. Viswanath, E. Jayamani, S. Siengchin, Influence of bio-based Kenaf polymer composites on mechanical and acoustic properties for futuristic applications: an initiative towards net-zero carbon emissions, Polym. Test 134 (2024) 108409-108409, doi:10.1016/j.polymertesting.2024.108409.

[26] J.M.A. de Kort, F. Gauvin, M. Loomans, H.J.H Brouwers, Emission rates of bio-based building materials, A method description for qualifying and quantifying voc emissions, Sci. Total Env. 905 (2023) 167158-167158, doi:10.1016/j.scitotenv.2023.167158.

[27] H. Rodríguez-Tobías, J. Uzcátegui-Flores, Francisco Javier Enríquez-Medrano, G. Morales, Alma Gisela Martínez-Arellano, Further investigation on fatty acids-based methacrylate monomers: high temperature radical polymerization for obtaining copolymers and their blends with medium-oil alkyd resin for coatings, Prog. Org. Coat. 186 (2023) 107962-107962, doi:10.1016/j.porgcoat.2023.107962.

[28] A. Alrahlah, A.-B. Al-Odayni, Waseem Sharaf Saeed, Naaser A.Y. Abduh, R. Khan, A. Alshabib, Faisal Fahad N. Almajhdi, Riad M. Alodeni, Merry Angelyn Tan De Vera, Influence of Eugenol and its novel methacrylated derivative on the polymerization degree of resin-based composites, Polym. (Basel) 15 (5) (2023) 1124-1124, doi:10.3390/polym15051124.

[29] Dominika N. Lastovickova, Faye R. Toulan, Joshua R. Mitchell, D. VanOosten, A. Clay, Joseph F. Stanzione, Giuseppe R. Palmese, John J.La Scala, Resin, cure, and polymer properties of photopolymerizable resins containing scpbio-derived/scp isosorbide, J. Appl. Polym. Sci. 138 (25) (2021) app50574, doi:10.1002/app.50574.

[30] Y. Zhang, Y. Li, Vijay Kumar Thakur, L. Wang, J. Gu, Z. Gao, B. Fan, Q. Wu, Michael R. Kessler, Bio-based reactive diluents As sustainable replacements for styrene In Maeso resin, RSC Adv. 8 (25) (2018) 13780–13788, doi:10.1039/c8ra00339d.

[31] V. Jašek, S. Figalla, Vegetable oils for material applications – Available biobased compounds seeking their utilities, ACS Polym. Au 5 (2) (2025) 105–128, doi:10.1021/acspolymersau.5c00001.

[32] Md Abdullah Al Mahmud, Alexandra V. Aucoin, John A. Pojman, Bubble-free frontal polymerization of acrylates using 1,1,2,2-tetraphenyl-1,2-ethanediol As A free-radical initiator, J. Polym. Sci. 63 (14) (2025) 2853–2861, doi:10.1002/pol.20250433.

[33] C. Liu, J. Wen, G. Ma, Z. Wu, J. Qu, Bio-based uv-curable non-isocyanate urethane-functional acrylates coating with enhanced anti-smudge and anti-graffiti performance, Chem. Eng. J. 521 (2025) 166543-166543, doi:10.1016/j.cej.2025.166543.

[34] S. Figalla, V. Jašek, J. Fučík, P. Menčík, R. Přikryl, Poly(Lactide) upcycling approach through transesterification for stereolithography 3D printing, Biomacromolecules 25 (10) (2024) 6645–6655, doi:10.1021/acs.biomac.4c00840.

[35] P. Spasojević, Sanja I. Šešlija, Maja D. Marković, O. Pantić, Katarina M. Antić, M. Spasojević, Optimization of reactive diluent for bio-based unsaturated polyester resin: a rheological and thermomechanical study, Polym. (Basel) 13 (16) (2021) 2667-2667, doi:10.3390/polym13162667.

[36] A. Jagtap, Aarti P. More, Developments In reactive diluents: a review, Polym. Bull. 79 (8) (2021) 5667–5708, doi:10.1007/s00289-021-03808-5.

[37] Danielle A. Baguley, D. Bard, Geoffrey M. Evans, P.S. Monks, Rebecca L. Cordell, An experimental study of volatile organic compound (Voc) emissions from A resin 3D printer to assess exposure and exposure mitigation, ACS Chem. Health Saf. (2025), doi:10.1021/acs.chas.5c00167.

[38] P. Majgaonkar, R. Hanich, F. Malz, R. Brüll, Chemical recycling of post-consumer pla waste for sustainable production of ethyl lactate, Chem. Eng. J. 423 (2021) 129952, doi:10.1016/j.cej.2021.129952.

[39] Yee Heng Ho, A. Parthiban, Min Chyong Thian, Zhen Hong Ban, P. Siwayanan, Acrylated biopolymers derived via epoxidation and subsequent acrylation of vegetable oils, Int. J. Polym. Sci. 2022 (2022) 1–12, doi:10.1155/2022/6210128.

[40] R. Saraswat, S. Shagun, A. Dhir, A.S.S. Balan, S. Powar, M. Doddamani, Synthesis and application of sustainable vegetable oil-based polymers In 3D printing, RSC Sustain. 2 (6) (2024) 1708–1737, doi:10.1039/d4su00060a.

[41] S. Briede, T. Biemans, O. Platnieks, S. Gaidukovs, Tailored uv-curable acrylated linseed oil-based alkyds: optimizing crosslinking and coating performance through functionalization and reactive diluent design, Polym. (Guildf) 323 (2025) 128227-128227, doi:10.1016/j.polymer.2025.128227.

[42] W. Maaßen, S. Oelmann, D. Peter, W. Oswald, N. Willenbacher, Michaël A.R. Meier, Novel insights into pressure-sensitive adhesives based on plant oils, Macromol. Chem. Phys. 216 (15) (2015) 1609–1618, doi:10.1002/macp.201500136.

[43] J. Liu, X. Zou, F. Liu, J. Wang, J. Liu, X. Zou, F. Liu, J. Wang, Synthesis of rosin-modified epoxy soybean oil acrylates and its uv curing properties, J. Coat. Technol. Res. (2025) 1–15, doi:10.1007/s11998-025-01178-5.

[44] L. Phutthatham, P. Chaiyasat, H. Minami, A. Chaiyasat, Fabrication of bio-based polymer microcapsule containing fragrances via interfacial photo-initiated crosslinking, Int. J. Polym. Mater. 74 (9) (2024) 763–772, doi:10.1080/00914037.2024.2375344.

[45] T. Jessewitsch, N. Saou, L. Steinlein, K. Bensberg, Stefan F. Kirsch, G. Delaittre, Oleanolic acid-derived high-glass-transition-temperature methacrylic polymers, ACS Sustain. Chem. Eng. 12 (52) (2024) 18499–18507, doi:10.1021/acssuschemeng.4c05259.

[46] L. Shao, Y.-C. Chang, B. Zhao, X. Yan, Brian J. Bliss, M. Fei, C. Yu, J. Zhang, Bona fide upcycling strategy of anhydride cured epoxy and reutilization of decomposed dual monomers into multipurpose applications, Chem. Eng. J. 464 (2023) 142735-142735, doi:10.1016/j.cej.2023.142735.

[47] A. Farhadian, Mohammed A. Khelkhal, A. Tajik, Semen E. Lapuk, M. Rezaeisadat, A.A. Ескин, Nikolay O. Rodionov, Alexey V. Vakhin, Effect of Ligand structure on the kinetics of heavy oil oxidation: toward biobased oil-soluble catalytic systems for enhanced oil recovery, Ind. Eng. Chem. Res. 60 (41) (2021) 14713–14727, doi:10.1021/acs.iecr.1c03276.

[48] C. Li, M. Zhang, Z. Li, L. Li, Y. Wang, Y. Shi, Y. Xu, Z. Zhu, N. Shi, K. Guo, Fully bio-based epoxy resins from bisphenols of coumaroyl amide structure from Lignin derived vanillin and tyramine, Int. J. Biol. Macromol. 333 (Pt 2) (2025) 148792-148792, doi:10.1016/j.ijbiomac.2025.148792.

[49] T. Chen, L. Zhang, Y. Chen, R. Qiu, W. Liu, Non-isothermal curing kinetics of soybean oil-based resins: effect of initiator and reactive diluent, Prog. Org. Coat. 188 (2024) 108178-108178, doi:10.1016/j.porgcoat.2023.108178.

[50] Muhammad Abdur Rashid, S. Zhu, Q. Jiang, Y. Wei, W. Liu, Developing easy processable, recyclable, and self-healable biobased epoxy resin through dynamic covalent imine bonds, ACS Appl. Polym. Mater. 5 (1) (2022) 279–289, doi:10.1021/acsapm.2c01501.

[51] Y. Zhang, Q.-yang; Lei, S. Zhang, L. Dai, B. Lyu, L. Liu, Biobased unsaturated polyester thermosets from Castor oil and isosorbide with life cycle assessment, ACS Sustain. Chem. Eng. 13 (1) (2024) 374–385, doi:10.1021/acssuschemeng.4c07624.

[52] T. Chen, C. Su, Y. Zeng, Y. Chen, R. Qiu, W. Liu, Effects of hydrogen bonds on soybean oil-based thermosets and their bamboo fibers composites, Compos. Commun. 33 (2022) 101231-101231, doi:10.1016/j.coco.2022.101231.

[53] A. Mishra, M. Sonowal, Venkata Yasaswy Turlapati, P. Maiti, B.C Meikap, A comprehensive thermo-kinetics devolatilization analysis of waste motor oil: thermal degradation kinetics, kinetic model, thermodynamic analysis, and ann, Int. J. Green Energy 20 (11) (2022) 1191–1203, doi:10.1080/15435075.2022.2155825.

[54] M. Bodor, A. Lasagabáster-Latorre, G. Arias-Ferreiro, S. Dopico, M.J. Abad, Improving the 3D printability and mechanical performance of biorenewable soybean oil-based photocurable resins, Polym. (Basel) 16 (7) (2024) 977-977, doi:10.3390/polym16070977.

[55] M. Fei, T. Liu, B. Zhao, A. Otero, Y.-C. Chang, J. Zhang, From glassy plastic to ductile elastomer: vegetable oil-based uv-curable vitrimers and their potential use In 3D printing, ACS Appl. Polym. Mater. 3 (5) (2021) 2470–2479, doi:10.1021/acsapm.1c00063.

[56] Z. Weng, X. Huang, S. Peng, L. Zheng, L. Wu, 3D Printing of ultra-high viscosity resin by A linear scan-based vat photopolymerization system, Nat. Commun. 14 (1) (2023) 4303-4303, doi:10.1038/s41467-023-39913-4.

[57] X. Feng, Q. Wang, Z. Yang, X. Liu, Kinetics analysis of radical photopolymerizations for uv-curable nanocomposites based on cellulose nanocrystals: promoting and enhancing mechanisms, Int. J. Biol. Macromol. 287 (2025) 138700, doi:10.1016/j.ijbiomac.2024.138700.

[58] J.A. Adeyera, J.A. Conti Silva, K. Kardel, R.L. Quirino, Effect of carbon–Carbon double bond content on the final properties of stereolithography 3D-printed parts from vegetable oil-based, acrylated resins, ACS Omega 10 (43) (2025) 51322–51334, doi:10.1021/acsomega.5c06728.

[59] A.M. Herrera-González, M. Caldera-Villalobos, A.A. Pérez-Mondragón, C.E. Cuevas-Suárez, J.A. González-López, Analysis of double bond conversion of photopolymerizable monomers by ftir-atr spectroscopy, J. Chem. Educ. 96 (8) (2019) 1786–1789, doi:10.1021/acs.jchemed.8b00659.

[60] J. Grimalt, L. Frattini, P. Carreras, V. Fombuena, Optimizing rheological performance of unsaturated polyester resin with bio-based reactive diluents: a comprehensive analysis of viscosity and thermomechanical properties, Polym. Test 129 (2023) 108264, doi:10.1016/j.polymertesting.2023.108264.

[61] W. Liu, T. Xie, R. Qiu, Biobased thermosets prepared from rigid isosorbide and flexible soybean oil derivatives, ACS Sustain. Chem. Eng. 5 (1) (2016) 774–783, doi:10.1021/acssuschemeng.6b02117.

[62] S. Briede, O. Platnieks, M. Dārziņa, A. Jirgensons, S. Gaidukovs, Effect of novel furan-based ester reactive diluent on structure and properties of scpuv/scp-crosslinked acrylated rapeseed oil, J. Polym. Sci. 61 (24) (2023) 3318–3328, doi:10.1002/pol.20230451.

[63] E. Hernández, Mirna A. Mosiewicki, Norma E. Marcovich, Bio-based polymers obtained from modified fatty acids and soybean oil with tailorable physical and mechanical performance, Eur. J. Lipid Sci. Technol. 122 (10) (2020), doi:10.1002/ejlt.202000182.

[64] Y. Liu, C. Li, J. Dai, Y. Jiang, X. Liu, J. Zhu, Synthesis of multifunctional monomers from Rosin for the properties enhancement of soybean-oil based thermosets, Sci. China Technol. Sci. 60 (9) (2017) 1332–1338, doi:10.1007/s11431-016-0777-5.

[65] C. Zhang, M. Yan, Eric W. Cochran, Michael R. Kessler, Biorenewable polymers based on acrylated epoxidized soybean oil and methacrylated vanillin, Mater. Today Commun. 5 (2015) 18–22, doi:10.1016/j.mtcomm.2015.09.003.

[66] C. Ventura-Hunter, V. Lechuga-Islas, J. Ulbrich, C. Kellner, Ulrich S. Schubert, E. Saldívar-Guerra, M. Rosales-Guzmán, C. Guerrero-Sánchez, Glycerol methacrylate-based copolymers: reactivity ratios, physicochemical characterization and cytotoxicity, Eur. Polym. J. 178 (2022) 111478-111478, doi:10.1016/j.eurpolymj.2022.111478.

[67] Li Yong Jiao, G. Yuan, Y. Qi, Lin Lin Li, Synthesis and properties of polyacrylate emulsion modified by pentaerythritol tetraacrylate, Adv. Mat. Res. 781-784 (2013) 550–553, doi:10.4028/www.scientific.net/amr.781-784.550.

[68] Gan, Y.; Jiang, X. Photo-cured materials from vegetable oils; 2014; pp 1–27. https://doi.org/10.1039/9781782621850-00001.

[69] S. Grishchuk, J. Karger-Kocsis, Hybrid thermosets from vinyl ester resin and acrylated epoxidized soybean oil (Aeso), Express Polym. Lett. 5 (1) (2010) 2–11, doi:10.3144/expresspolymlett.2011.2.